



NMR Characterization of Rearranged Staurosporine Aglycone Analogues from the Marine Sponge *Damiria* sp.

Trong D. Tran^{1,†}, Laura K. Cartner^{1,2}, Heidi R. Bokesch^{1,2}, Curtis J. Henrich^{1,2}, Xin W. Wang³, Chulabhorn Mahidol^{4,5}, Somsak Ruchirawat^{4,5,6}, Prasat Kittakoop^{4,5,6}, Barry R. O'Keefe¹, Kirk R. Gustafson¹

¹Molecular Targets Program, Center of Cancer Research, National Cancer Institute, Frederick, Maryland 21701-1201, United States ²Basic Science Program, Leidos Biomedical Research, Inc., Frederick National Laboratory for Cancer Research sponsored by the National Cancer Institute, Frederick, Maryland 21702-1201, United States ³Laboratory of Human Carcinogenesis, Center for Cancer Research, National Cancer Institute, Bethesda, Maryland 20892, United States ⁴Chulabhorn Research Institute, Kamphaeng Phet 6 Road, Laksi, Bangkok 10210, Thailand ⁵Chulabhorn Graduate Institute, Chemical Biology Program, Chulabhorn Royal Academy, Kamphaeng Phet 6 Road, Laksi, Bangkok 10210, Thailand ⁶Center of Excellence on Environmental Health and Toxicology (EHT), CHE, Ministry of Education, Bangkok, Thailand

Abstract

The indolocarbazole family of bisindole alkaloids is best known for the natural product staurosporine, a protein kinase C inhibitor that belongs to the indolo[2,3-*a*]carbazole structural class. A large number of other indolo[2,3-*a*]carbazoles have subsequently been isolated and identified, but other isomeric forms of indolocarbazole natural products have rarely been reported. An extract of the marine sponge *Damiria* sp., which represents an understudied genus, provided two novel alkaloids named damirines A (**1**) and B (**2**). Their structures were assigned by comprehensive NMR spectroscopic analyses, and for compound **2** this included application of the LR-HSQMBC pulse sequence, a long-range heteronuclear correlation experiment that has particular utility for defining proton-deficient scaffolds. The damirines represent a new hexacyclic carbon-nitrogen framework comprised of an indolo[3,2-*a*]carbazole fused with either an aminoimidazole or a imidazolone ring. Compound **1** showed selective cytotoxic properties toward six different cell lines in the NCI-60 cancer screen.

Keywords

Indolocarbazole; LR-HSQMBC; *Damiria*; damirine

Correspondence: Kirk Gustafson, Molecular Targets Program, Center for Cancer Research, NCI-Frederick, Build. 562, Rm. 201, Frederick, Maryland 21702, USA, gustafki@mail.nih.gov.

[†]Current address: GeneCology Research Centre, University of the Sunshine Coast, Maroochydore DC, Queensland 4558, Australia

SUPPORTING INFORMATION

Additional supporting information may be found online in the Supporting Information section at the end of the article.

1 INTRODUCTION

The indolocarbazole family of alkaloids has been the focus of numerous drug discovery and development studies since staurosporine (**3**), an indolo[2,3-*a*]carbazole compound joined with an amino sugar residue, was isolated in 1977^[1] and subsequently found to exhibit a wide range of biological activities including inhibition of protein kinase C, along with cytotoxic, antimicrobial, and anti-parasitic activities.^[2] Structurally, the indolocarbazoles are carbon-nitrogen heterocycles characterized by an indole unit fused to one of the benzenoid rings of a carbazole moiety.^[3] Five indolocarbazole isomers are defined based on the position and orientation of the indole and carbazole ring fusion, including indolo[2,3-*a*]carbazole, indolo[3,2-*a*]carbazole, indolo[3,2-*b*]carbazole, indolo[2,3-*b*]carbazole and indolo[2,3-*c*]carbazole.^[3-4] Over the last 40 years, almost all of the indolocarbazoles isolated from nature are indolo[2,3-*a*]carbazoles, therefore interest in the chemistry and pharmacology of these alkaloids has been primarily focused on this structural class. The other indolocarbazole isomers have received only limited attention.^[4]

The marine sponge genus *Damiria* has rarely been investigated chemically, and the only compounds previously reported from a *Damiria* sponge are the pyrroloquinoline alkaloids damirones A and B.^[5] Fractionation of the organic solvent extract of a collection of *Damiria* sp. made in Thailand provided two novel compounds, damirines A (**1**) and B (**2**), which belong to the indolo[3,2-*a*]carbazole class. Although the indolocarbazole scaffolds have been synthesized since the 1950s,^[6] the first natural indolo[3,2-*a*]carbazole, ancorinazole, was reported from the New Zealand sponge *Ancoina* sp. in 2002.^[7] Three additional members of this class were described in 2013, including asteropusazoles A and B from the Bahamas sponge *Asteropus* sp.,^[8] and racemosin B from the Chinese green alga *Caulerpa racemosa*.^[9] This paper describes the structure elucidation and comprehensive NMR characterization of the sponge metabolites damirines A (**1**) and B (**2**), including utilization of long-range heteronuclear correlation data from HMBC and LR-HSQMBC experiments optimized for small ¹H-¹³C couplings.^[10]

2 RESULTS AND DISCUSSION

The *Damiria* sp. extract was active in an assay for growth inhibition against EpCAM(+) hepatocellular carcinoma cells so it was selected for further chemical study.^[11] Sequential chromatography of the extract on a diol solid phase extraction (SPE) support, followed by C₁₈ reversed-phase HPLC provided damirines A (**1**) and B (**2**).

Damirine A (**1**) was purified as an optically inactive brown amorphous powder. Its molecular formula was established as C₁₉H₁₃N₅ based on (+)-HRESIMS data, which required 16 degrees of unsaturation. The UV spectrum of **1** revealed absorption maxima at $\lambda = 213, 243, 271, 293, 307$ and 340 nm, consistent with extended conjugation of a polycyclic aromatic molecule. The highly aromatic character of **1** was further confirmed by the presence of only sp² carbons in the ¹³C NMR spectrum, with chemical shifts between 101.4 and 153.0 ppm (Table 1). The gCOSY spectrum revealed two sets of ABCD proton-proton spin systems [δ_{H} 7.55 (d, $J = 7.8$ Hz), 7.30 (dd, $J = 7.2, 7.8$ Hz), 7.24 (t, $J = 7.2$ Hz) and 8.57 (d, $J = 7.2$ Hz)] and [δ_{H} 7.62 (d, $J = 7.8$ Hz), 7.29 (dd, $J = 7.2, 7.8$ Hz), 7.19 (dd, $J = 7.2, 7.8$ Hz) and 8.44

(d, $J = 7.8$ Hz)]. HMBC correlations for these aromatic protons and for two exchangeable protons NH-8 (δ_{H} 11.86) and NH-13 (δ_{H} 11.51) were consistent with the presence of two 2,3-disubstituted-indole moieties (Table 1). A key ROESY correlation between H-12/NH-13 and a four-bond HMBC correlation for NH-13/C-7b that was observed when the pulse sequence was optimized for long-range correlations (${}^nJ_{\text{CH}} = 3$ Hz), established a linkage between C-12b and C-12c (Figure 2). The long-range optimized HMBC experiment also showed correlations from NH-8/C-4c and NH-8/C-7a, which helped define the fully substituted C ring in **1**. However, no other protons correlated with these two carbons and no correlations were observed with the remaining C-6 quaternary carbon. Consideration of the characteristic downfield ${}^{13}\text{C}$ chemical shift (δ_{C} 153.0) in the remaining CH_3N_3 moiety, and the requirement for two more unsaturation equivalents in **1**, suggested that the last structural component was an amino-substituted imidazole ring. Thus, the hexacyclic structure of **1** was assigned as an indolo[3,2-*a*]carbazole with an imidazole (ring F) fused on ring C. Comparison of experimentally measured δ_{C} values with carbon chemical shifts calculated by density functional theory (DFT) methods (Table 2) provided additional support for the assigned structure of damirine A (**1**).

Damirine B (**2**) was isolated as a brown powder with a molecular formula established by (+)-HRESIMS measurements of $\text{C}_{19}\text{H}_{12}\text{N}_4\text{O}$. The ${}^1\text{H}$ and ${}^{13}\text{C}$ NMR data of **2** (Table 3) were very similar to those recorded for **1**, except for the presence of two additional exchangeable protons at δ_{H} 11.32 and 11.82, corresponding to NH-5 and NH-7, respectively. The ${}^1\text{H}$ - ${}^{15}\text{N}$ HSQC spectrum confirmed the presence of four readily observable NH protons in **2**. Following extensive 1D and 2D NMR analyses, the same indolo[3,2-*a*]carbazole scaffold found in **1** was confirmed in damirine B (**2**). Key HMBC correlations including those from NH-8 and NH-13 helped define the fused B, C, and D rings of the indolocarbazole system, while a ROESY between H-12 and NH-13 revealed the relative orientation of the two indoles. The molecular formula of **2** required the addition of oxygen and the loss of NH relative to the molecular formula of **1**. This was consistent with replacement of the ring F amine substituent in **1**, whose NH protons were never observable, with a carbonyl group to give an imidazolone moiety in **2**, with NH protons that were facile to observe in $\text{DMSO-}d_6$. HMBC correlations from NH-5 and NH-7 in ring F to C-4c, C-7a and the C-6 carbonyl (δ_{C} 155.8), along with a ROESY correlation between H-4 and NH-5 supported this assignment. Application of the recently described LR-HSQMBC NMR pulse sequence provided further evidence for the structure of damirine B (**2**).^[10] The LR-HSQMBC experiment facilitates detection of long-range (4-bond and 5-bond) heteronuclear couplings that generally are not observed in HMBC spectra, so it has particular utility in structural studies of proton-deficient scaffolds. It has been successfully employed in several structural studies of novel natural products, which illustrated the importance of the additional heteronuclear correlations this technique can provide.^[12] A ${}^1\text{H}$ - ${}^{13}\text{C}$ LR-HSQMBC experiment with **2** (optimized for ${}^nJ_{\text{CH}} = 2$ Hz) provided a number of additional 4-bond correlations, including a key one from NH-13 to C-4c, that reinforced the structure assigned to damirine B (**2**).

Damirine A (**1**) showed modest growth inhibitory activity against Hep3B (EpCAM-positive) hepatocellular carcinoma cells, thus compounds **1** and **2** were subsequently screened for growth inhibitory activity in the NCI-60 cell line anticancer screen.^[13] Damirine A (**1**) was

sufficiently active to be selected for full 5-dose testing against all 60 cancer cell lines, where it exhibited selective cytotoxic activity and was most effective at inhibiting the growth of one melanoma (MALME-3M, 50% growth inhibition, $GI_{50} = 1.9 \mu\text{M}$), one breast (MDA-MB-468, $GI_{50} = 2.0 \mu\text{M}$), two colon (SW-620, $GI_{50} = 3.3 \mu\text{M}$; HCC-2998, $GI_{50} = 2.3 \mu\text{M}$), and two leukemia (MOLT-4, $GI_{50} = 1.9 \mu\text{M}$; K-562, $GI_{50} = 2.2 \mu\text{M}$) cell lines (see Supporting Information).

3 CONCLUSIONS

Damirines A (**1**) and B (**2**) were isolated from the sponge *Damiria* sp. and their structures were unambiguously solved using a combination of NMR methodologies. The sparse distribution of observable protons in the core of these novel hexacyclic bisindole alkaloids necessitated the acquisition of long-range (> three bonds) ^1H - ^{13}C heteronuclear correlation data. Two different experimental approaches were employed, one using HMBC optimized for 3 Hz couplings, and the other using the LR-HSQMBC pulse sequence optimized for 2 Hz couplings, to obtain the desired spectroscopic data. These long-range correlations allowed assignment of damirine A (**1**) as an indolo[3,2-*a*]carbazole fused to an aminoimidazole ring, while damirine B (**2**) had the same indolocarbazole core fused to an imidazolone moiety. While the indolo[3,2-*a*]carbazole scaffold has been generated in prior synthetic studies,^[6, 14] it has only rarely been found in a natural product. Damirines A (**1**) and B (**2**) provide new carbon-nitrogen skeletons not seen in any other reported secondary metabolites, and damirine A (**1**) exhibited selective growth inhibitory effects against six different cancer cell lines.

4 EXPERIMENTAL PART

NMR spectra were obtained with a Bruker Avance III NMR spectrometer equipped with a 3 mm TCI $^1\text{H}/^{13}\text{C}/^{15}\text{N}$ cryogenic probe and operating at 600 MHz for ^1H and 150 MHz for ^{13}C . Spectra were calibrated to residual solvent signals at $\delta_{\text{H}} 2.50$ and $\delta_{\text{C}} 39.5$ (DMSO- d_6). HMBC experiments were optimized for $^nJ_{\text{CH}} = 8.3$ Hz, unless otherwise indicated. ^{15}N assignments were based on ^1H - ^{15}N HSQC correlations with $^1J_{\text{NH}} = 90$ Hz. The δ_{N} values were not calibrated to an external standard but were referenced to neat NH_3 ($\delta 0.00$) using the standard Bruker parameters. The ^1H - ^{13}C LR-HSQMBC experiment was optimized for $^nJ_{\text{C,H}} = 2.0$ Hz, with 768 increments in the f1 dimension. Preparative reversed-phase HPLC was performed on an Agilent 1260 Infinity HPLC or a Gilson PLC system using a Phenomenex Luna-C₁₈ (5 μ , 100 \AA , 250 \times 10 mm) column with the indicated gradient. UV and IR spectra were measured with a Thermo Scientific Nanodrop 2000C spectrophotometer and a Bruker ALPHA II FT-IR spectrometer, respectively. (+)-HRESIMS data were acquired on an Agilent Technology 6530 Accurate-mass Q-TOF LC/MS.

Specimens of the sponge *Damiria* sp. were collected around Phuket Island, Thailand in April 2014, under contract through the Coral Reef Research Foundation for the Natural Products Branch, National Center Institute. A voucher specimen (voucher ID # OYYA1139; NSC # C034303) was deposited at the Smithsonian Institute, Washington, D.C. The sponge sample (683 g, wet weight) was extracted according to the procedures detailed by McCloud to give 2.62 g of organic solvent (CH_2Cl_2 -MeOH, 1:1 and 100% MeOH) extract.^[15] A portion of

the organic extract (900 mg) was fractionated on diol SPE cartridges (2 g) eluting with 9:1 hexane-CH₂Cl₂, 20:1 CH₂Cl₂-EtOAc, 100% EtOAc, 5:1 EtOAc-MeOH, and 100% MeOH in a stepwise manner. Final purification was achieved by C₁₈ HPLC of the MeOH fraction (347.2 mg) with a linear H₂O/CH₃CN gradient (0.1% formic acid) from 10 to 50% CH₃CN over 22 minutes to give a total of 9.2 mg of damirine A (**1**) and 2.4 mg of damirine B (**2**). An additional 1.2 mg of **1** (TFA salt) was obtained by C₁₈ HPLC eluted with a linear H₂O/CH₃CN gradient (0.5% TFA) from 40 to 50% CH₃CN over 20 minutes.

Damirine A (1): brown solid; UV (MeOH) λ_{\max} (log ϵ) 213 (5.27), 243 (5.36), 271 (5.40), 293 (5.26), 307 (5.23), 340 (4.72); IR (neat) ν_{\max} 3305 (br), 1681, 1581, 1380, 1349, 1264 cm⁻¹; ¹H and ¹³C NMR data, Table 1; HRESIMS m/z 312.1249 [M + H]⁺ (calcd for C₁₉H₁₄N₅, 312.1244).

Damirine B (2): brown solid; UV (MeOH) λ_{\max} (log ϵ) 215 (4.88), 244 (4.88), 269 (4.91), 288 (4.78), 340 (4.22), 355 (4.32); IR (neat) ν_{\max} 3340 (br), 1643, 1370, 1281 cm⁻¹; ¹H and ¹³C NMR data, Table 3; HRESIMS m/z 313.1081 [M + H]⁺ (calcd for C₁₉H₁₃N₄O, 313.1084).

Computational Details.

Molecular mechanics were performed using MacroModel interfaced to the Maestro program (Version 2015.3, *Schrödinger*). Conformational searches used the OPLS_2005 force field. Only one conformer was found within 3 kcal/mol of internal relative energies. The conformer was then subjected to geometry optimization in DMSO solution on Gaussian 09 at the DFT level with the B3LYP functional and the 6-31G(d) basis set. Single point calculations in DMSO with the B3LYP functional and the 6-311G(d,p) basis set were then employed to provide the shielding constants of carbon and proton nuclei. Meanwhile, the same procedure was applied on tetramethylsilane (TMS) and benzene. The theoretical chemical shifts were calculated using the equation $\delta_{\text{calc}}^x = \sigma_{\text{ref}} - \sigma^x + \delta_{\text{ref}}$, where δ_{calc}^x is the calculated chemical shift for nucleus x; σ^x is the shielding constant for nucleus x; σ_{ref} and δ_{ref} are the shielding constant and chemical shift of the reference compound (TMS or benzene) computed at the same level of theory.^[16] Calculated shielding constants of references in DMSO are $\sigma_{\text{TMS}}^{\text{C}} = 184.70015$, $\sigma_{\text{benzene}}^{\text{C}} = 49.37645$, $\sigma_{\text{TMS}}^{\text{H}} = 31.94609$ and $\sigma_{\text{benzene}}^{\text{H}} = 24.26277$ ppm; Chemical shifts of references in DMSO are $\delta_{\text{TMS}}^{\text{C}} = 0$, $\delta_{\text{benzene}}^{\text{C}} = 128.3$, $\delta_{\text{TMS}}^{\text{H}} = 0$ and $\delta_{\text{benzene}}^{\text{H}} = 7.37$ ppm.^[17] Systematic errors during the chemical shift calculation were removed by empirical scaling according to $\delta_{\text{calc}}^* = (\delta_{\text{calc}} - b)/a$; where the slope (a), the intercept (b) and the correlation coefficient (R^2) were determined from a plot of δ_{calc} against δ_{exp} . The mean absolute error (MAE) was defined as

$\sum_{i=1}^n |\delta_{\text{calc}} - \delta_{\text{exp}}|/n$. The corrected mean absolute error (CMAE) was defined as

$$\sum_{i=1}^n |\delta_{\text{calc}}^* - \delta_{\text{exp}}|/n.[18]$$

Supplementary Material

Refer to Web version on PubMed Central for supplementary material.

ACKNOWLEDGMENTS

We thank the National Research Council of Thailand (NRCT) for permission of research operations in Thailand and the Department of National Parks, Wildlife and Plant Conservation for permission and organization of the sample collection. Grateful acknowledgement goes to the Natural Products Support Group (NCI at Frederick) for extract preparation. This research was supported in part by the Intramural Research Program of the NIH, National Cancer Institute, Center for Cancer Research and with federal funds from the National Cancer Institute, National Institutes of Health, under contract HHSN261200800001E. This work utilized the computational resources of the NIH HPC Biowulf cluster. The content of this publication does not necessarily reflect the views or policies of the Department of Health and Human Services, nor does mention of trade names, commercial products, or organizations imply endorsement by the U.S. Government.

REFERENCES

- [1]. Omura S, Iwai Y, Hirano A, Nakagawa A, Awaya J, Tsuchiya H, Takahashi Y, Masuma R, J. Antibiot 1977, 30, 275.
- [2]. Nakano H, mura S, J. Antibiot 2009, 62, 17.
- [3]. Janosik T, Wahlström N, Bergman J, Tetrahedron 2008, 64, 9159.
- [4]. Janosik T, Rannug A, Rannug U, Wahlstrom N, Slatt J, Bergman J, Chem. Rev 2018, 118, 9058. [PubMed: 30191712]
- [5]. Stierle DB, Faulkner DJ, J. Nat. Prod 1991, 54, 1131.
- [6]. (a)Tomlinson ML, J. Chem. Soc 1951, 809–811;(b)Mann F, Willcox T, J. Chem. Soc 1958, 1525.
- [7]. Meragelman KM, West LM, Northcote PT, Pannell LK, McKee TC, Boyd MR, J. Org. Chem 2002, 67, 6671. [PubMed: 12227796]
- [8]. (a)Russell F, Harmody D, McCarthy PJ, Pomponi SA, Wright AE, J. Nat. Prod 2013, 76, 1989; [PubMed: 24063539] (b)Zheng X, Lv L, Lu S, Wang W, Li Z, Org. Lett 2014, 16, 5156. [PubMed: 25222652]
- [9]. Liu D-Q, Mao S-C, Zhang H-Y, Yu X-Q, Feng M-T, Wang B, Feng L-H, Guo Y-W, Fitoterapia 2013, 91, 15. [PubMed: 23978579]
- [10]. Williamson RT, Buevich AV, Martin GE, Parella T, J. Org. Chem 2014, 79, 3887. [PubMed: 24708226]
- [11]. Henrich CJ, Budhu A, Yu Z, Evans JR, Goncharova EI, Ransom TT, Wang XW, McMahon JB, Chem. Biol. Drug Des B2013B, 82, 131. [PubMed: 23879724]
- [12]. Some recent examples include:(a)Chan STS, Nani RR, Schauer EA, Martin GE, Williamson RT, Saurí J, Buevich AV, Schafer WA, Joyce LA, Goey AKL, Figg WD, Ransom TT, Henrich CJ, McKee TC, Moser A, MacDonald SA, Khan S, McMahon JB, Schnermann MJ, Gustafson KR, J. Org. Chem 2016, 81, 10631; [PubMed: 27934476] (b)Milanowski DJ, Oku N, Cartner LK, Bokesch HR, Williamson RT, Saurí J, Liu Y, Blinov KA, Ding Y, Li X-C, Ferreira D, Walker LA, Khan S, Davies-Coleman MT, Kelley JA, McMahon JB, Martin GE, Gustafson KR, Chem. Sci 2018, 9, 307. [PubMed: 29619201]
- [13]. Shoemaker RH, Nat. Rev. Cancer 2006, 6, 813. [PubMed: 16990858]
- [14]. (a)Sankar E, Raju P, Karunakaran J, Mohanakrishnan AK, J. Org. Chem 2017, 82, 13583; [PubMed: 29134811] (b)Kotha S, Saifuddin M, Aswar VR, Org. Biomol. Chem 2016, 14, 9868. [PubMed: 27714197]
- [15]. McCloud TG, Molecules 2010, 15, 4526. [PubMed: 20657375]
- [16]. Sarotti AM, Pellegrinet SC, J. Org. Chem 2009, 74, 7254. [PubMed: 19725561]
- [17]. Gottlieb HE, Kotlyar V, Nudelman A, J. Org. Chem 1997, 62, 7512. [PubMed: 11671879]
- [18]. (a)Smith SG, Goodman JM, J. Org. Chem 2009, 74, 4597; [PubMed: 19459674] (b)Smith SG, Goodman JM, J. Am. Chem. Soc 2010, 132, 12946. [PubMed: 20795713]

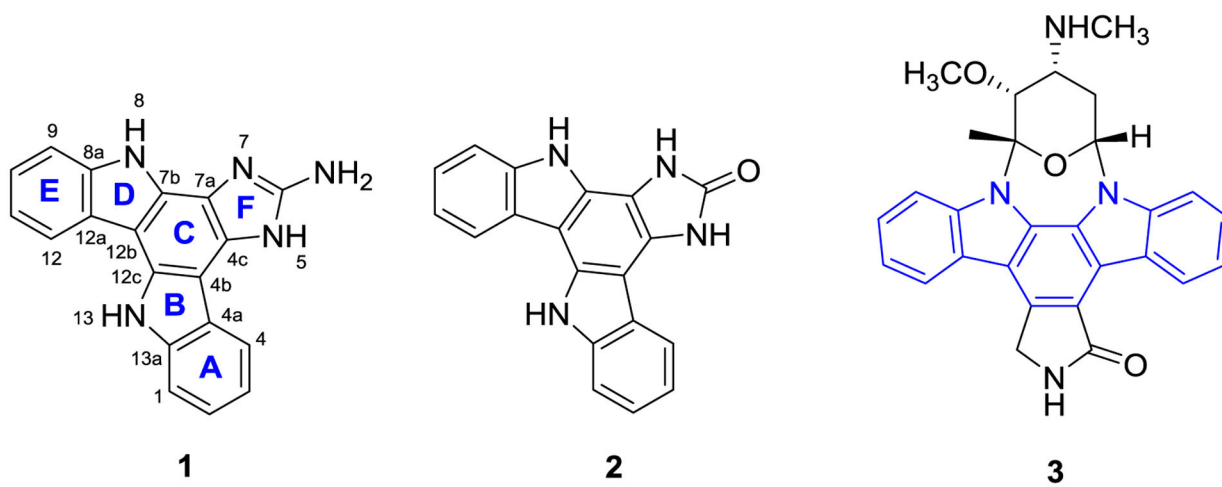


FIGURE 1.
Structures of damirines A (1) and B (2), and staurosporine (3)

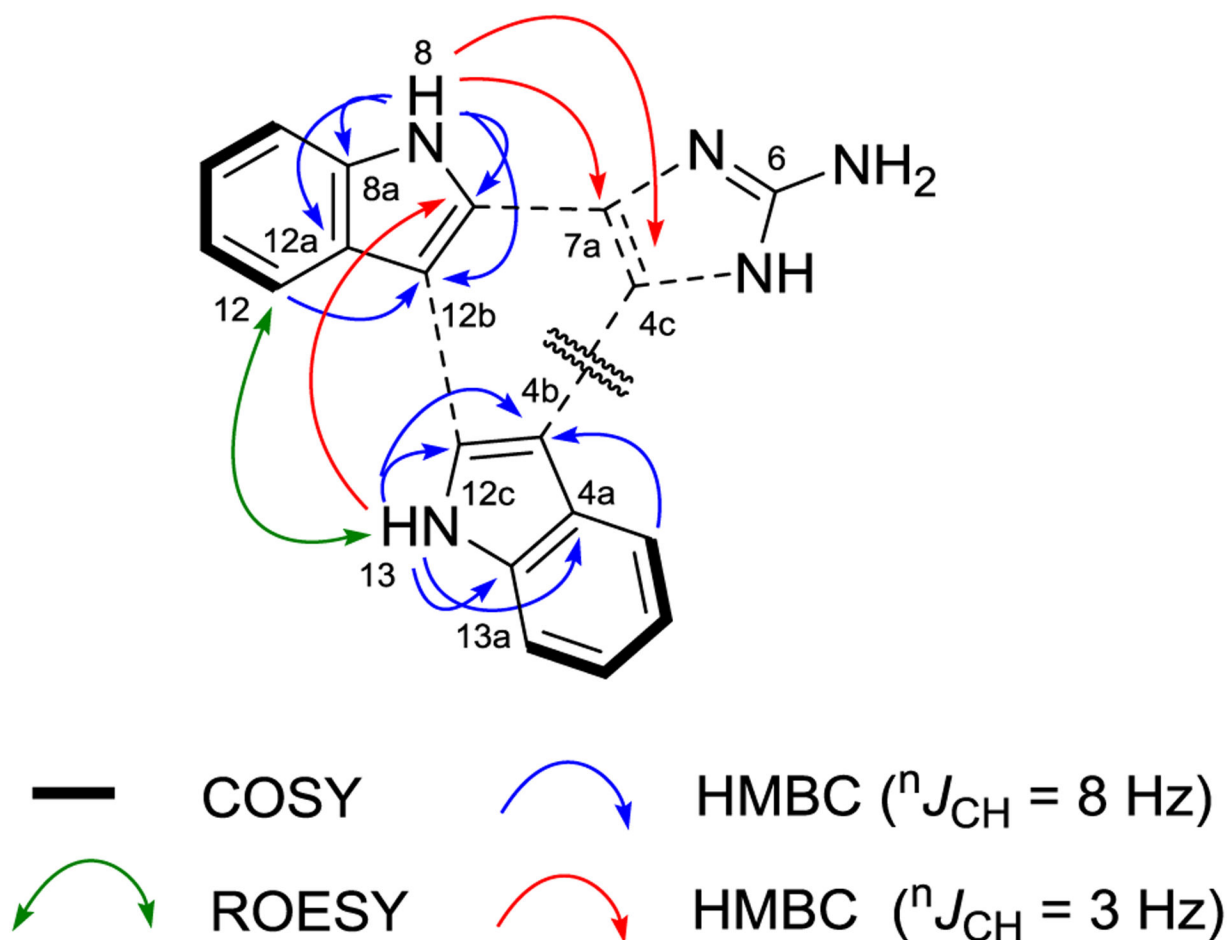


FIGURE 2.
Key COSY, HMBC, and ROESY correlations for damirine A (1)

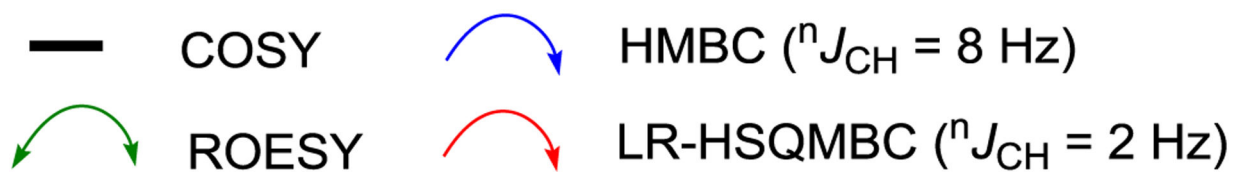
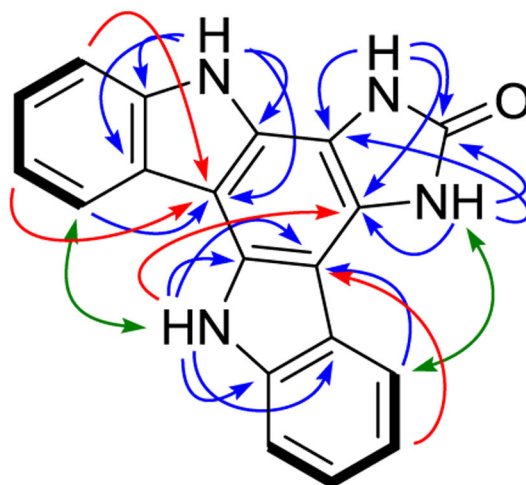


FIGURE 3.
Key COSY, HMBC, LR-HSQMBC, and ROESY correlations for damirine B (2)

TABLE 1.

NMR spectroscopic data (600 MHz ^1H , 150 MHz ^{13}C , DMSO- d_6) for damirine A (**1**)

Position	δ_{C} , type	δ_{H} (J in Hz)	ROESY	HMBC
1	110.6, CH	7.62, d (7.8)	13	3, 4a, 4b ^a , 13a ^a
2	122.2, CH	7.29, dd (7.2, 7.8)		1, 4, 13a, 4a ^a
3	118.4, CH	7.19, dd (7.2, 7.8)		1, 4, 4a, 4b ^a , 13a ^a
4	120.0, CH	8.44, d (7.8)		2, 4b, 13a, 1 ^a
4a	121.9, C			
4b	101.7, C			
4c	123.2, C			
5		<i>b</i>		
6	153.0, C			
7		<i>b</i>		
7a	116.7, C			
7b	127.8, C			
8		11.86, s	9	7b, 8a, 12a, 12b, 7a ^a , 4c ^a
8a	138.3, C			
9	110.7, CH	7.55, d (7.8)	8	11, 12a, 8a ^a , 12b ^a
10	122.4, CH	7.30, dd (7.2, 7.8)		8a, 9, 12, 12a ^a
11	118.5, CH	7.24, t (7.2)		9, 12, 12a, 8a ^a , 12b ^a
12	120.0, CH	8.57, d (7.2)	13	8a, 10, 12b, 9 ^a
12a	122.7, C			
12b	101.4, C			
12c	129.8, C			
13		11.51, s	1, 12	4a, 4b, 12c, 13a, 1 ^a , 7b ^a
13a	138.6, C			

^aObserved with $^nJ_{\text{CH}} = 3$ Hz.^bNot observed.

TABLE 2.Comparison of experimental and DFT calculated ^{13}C and ^1H chemical shifts in DMSO- d_6 for damirine A (**1**)

Position	δ_{C} (exp.)	δ_{C} (calc.)	δ_{H} (exp.)	δ_{H} (calc.)
1	110.6	108.9	7.62	7.63
2	122.2	122.5	7.29	7.31
3	118.4	118.6	7.19	7.19
4	120.0	119.1	8.44	8.41
4a	121.9	121.3		
4b	101.7	99.5		
4c	123.2	125.9		
6	153.0	150.2		
7a	116.7	122.7		
7b	127.8	129.1		
8a	138.3	138.5		
9	110.7	109.0	7.55	7.55
10	122.4	122.8	7.30	7.32
11	118.5	118.9	7.24	7.21
12	120.0	119.2	8.57	8.59
12a	122.7	123.1		
12b	101.4	100.2		
12c	129.8	130.1		
13a	138.6	138.2		
R ²		0.9759		0.9983

TABLE 3.NMR spectroscopic data (600 MHz ^1H , 150 MHz ^{13}C , DMSO- d_6) for damirine B (2)

Position	δ_{C} , type	δ_{N}^a	δ_{H} (J in Hz)	ROESY	HMBC
1	110.4, CH		7.61, d (7.8)	13	3, 4a
2	122.5, CH		7.30, t (7.8)		1, 4, 13a
3	118.3, CH		7.16, t (7.8)		1, 4a, 4 ^b , 4b ^b , 13a ^b
4	120.1, CH		8.48, d (7.8)	5	2, 4b, 13a
4a	121.5, C				
4b	100.0, C				
4c	120.7, C				
5		123.0	11.32, s	4	4c, 6, 7a
6	155.8, C				
7		117.3	11.82, s		4c, 6, 7a
7a	107.5, C				
7b	125.3, C				
8		118.2	12.73, s	9	7b, 8a, 12a, 12b
8a	138.8, C				
9	110.6, CH		7.55, d (7.8)	8	11, 12a, 12b ^b
10	122.5, CH		7.32, dd (7.2, 7.8)		8a, 9, 12, 12a ^b
11	118.3, CH		7.23, dd (7.2, 7.8)		9, 12a, 8a ^b , 12b ^b
12	120.0, CH		8.56, d (7.8)	13	8a, 10, 12b
12a	122.4, C				
12b	101.4, C				
12c	129.9, C				
13		116.6	11.56, s	1, 12	4a, 4b, 12c, 13a, 4c ^b
13a	138.7, C				

^aDetermined with ^1H - ^{15}N HSQC.^bObserved by LR-HSQMBC optimized for 2 Hz.